THE JOURNAL OF BIOLOGICAL CHEMISTRY VOL. 287, NO. 34, pp. 28656–28665, August 17, 2012

The Antiepileptic Drug Valproic Acid Restores T Cell Homeostasis and Ameliorates Pathogenesis of Experimental Autoimmune Encephalomyelitis*

Received for publication, February 26, 2012, and in revised form, June 20, 2012 Published, JBC Papers in Press, June 25, 2012, DOI 10.1074/jbc.M112.356584

Jie Lv[‡§1], Changsheng Du[‡1], Wei Wei[‡§], Zhiying Wu[¶], Guixian Zhao[¶], Zhenxin Li[¶], and Xin Xie[‡§2]

From the [‡]Shanghai Key Laboratory of Signaling and Disease Research, Laboratory of Receptor-based Bio-medicine, School of Life Sciences and Technology, Tongji University, Shanghai 200092, China, the [§]State Key Laboratory of Drug Research, the National Center for Drug Screening, Shanghai Institute of Materia Medica, Chinese Academy of Sciences, Shanghai 201203, China, and the [¶]Department of Neurology and Institute of Neurology, Huashan Hospital, Shanghai Medical College, Fudan University, Shanghai 200040, China

Background: Dysregulation of T cell survival and apoptosis is the common cause of autoimmune diseases including multiple sclerosis (MS).
Results: Valproic acid (VPA) treatment restores the dysregulated apoptosis of T cells and reduces the symptoms of EAE.
Conclusion: In addition to the antiepileptic activity, VPA also regulates T cell homeostasis.
Significance: As an orally available drug, VPA might be used to treat autoimmune diseases, such as MS.

Maintaining a constant number and ratio of immune cells is one critical aspect of the tight regulation of immune homeostasis. Breakdown of this balance will lead to autoimmune diseases such as multiple sclerosis (MS). The antiepileptic drug valproic acid (VPA) was reported to regulate the growth, survival, and differentiation of many cells. However, its function in T cell homeostasis and MS treatment remains unknown. In this study, VPA was found to reduce spinal cord inflammation, demyelination, and disease scores in experimental autoimmune encephalomyelitis, a mouse model of MS. Further study indicated that VPA induces apoptosis in activated T cells and maintains the immune homeostasis. This effect was found to be mainly mediated by the caspase-8/caspase-3 pathway. Interestingly, this phenomenon was also confirmed in T cells from normal human subjects and MS patients. Considering the long history of clinical use and our new findings, we believe VPA might be a safe and effective therapy for autoimmune diseases, such as multiple sclerosis.

The immune system protects the body from disease-causing microorganisms. Foreign antigen stimulation usually leads to specific immune responses characterized by immune cell activation, differentiation, proliferation, and inflammatory gene expression, all of which in turn lead to inflammation. After the removal of antigens, the immune system returns to its preactivation state, ready to respond to next wave of attacks (1). The strength and the duration of the immune responses must be tightly regulated to ensure the effective elimination of the antigen in question but no severe tissue damage or death of the organism. Maintaining a constant number and ratio of immune cells is one aspect of such tight regulation (2).

Multiple sclerosis (MS)[3] is an autoimmune disease characterized by the immune-mediated demyelination and neurodegeneration of the CNS (3). Experimental autoimmune encephalomyelitis (EAE) is an animal model that shares many pathological and histological similarities with MS. Although many mechanisms have been proposed for the pathogenesis of MS, including oxidative stress, excitotoxicity, autoimmunity, hormonal imbalance (4), etc., it is generally accepted that the overactivation of $CD4^+$ T cells, especially the T_H-1 and T_H-17 subpopulations, is the direct cause of this disease (5). Recently, $CD8^+$ T cells have also been implicated in the pathogenesis of MS (6, 7). Previous studies suggest two major ways to maintain immune homeostasis. The first way involves the inhibitory cytokines, which limit the strength of immune cell activation and expansion, such as TGF-β or IL-10 (8, 9). Up-regulation of IL-10 production by small molecules or repetitive antigen stimulation of effector T_H-1 cells in the presence of TGF-β has been reported to suppress EAE (10, 11). The second way is to control cell death. Molecules such as Fas, Bim, Bax, and the caspases-8 and -10 are critically involved (12, 13). A recent study reported that enhanced expression of *Bcl2* via β-arrestin 1-dependent epigenetic modification attenuated the death of activated $CD4^+$ T cells and thus led to a severe form of EAE (14).

Histone deacetylase inhibitors (HDACis) are compounds that interfere with the function of histone deacetylase, an important class of epigenetic modulators. HDACis such as valproic acid (VPA) have a long history of use in psychiatry and

* This work was supported by National Natural Science Foundation of China Grants 31000399, 31171348, 31071227, and 81100963, 973 Program Grant 2012CB910404), and the Ministry of Science and Technology of China Grant 2009ZX09302-001.
⌘ *Author's Choice*—Final version full access.
[1] These authors contributed equally to this work.
[2] To whom correspondence should be addressed: 189 Guo Shou Jing Rd., Shanghai 201203, China. Tel.: 86-21-50801313, Ext. 156; Fax: 86-21-50800721; E-mail: xxie@mail.shcnc.ac.cn.

[3] The abbreviations used are: MS, multiple sclerosis; VPA, valproic acid; EAE, experimental autoimmune encephalomyelitis; HDACi, histone deacetylase inhibitor; CFSE, carboxyfluorescein diacetate succinimidyl ester; Z-VAD-FMK, Z-Val-Ala-Asp (OMe)-fluoromethyl ketone; PBMC, peripheral blood mononuclear cell(s); PI, propidium iodide; ANOVA, analysis of variance.

neurology as mood stabilizers and anti-epileptics (15, 16). Recently, two HDACis, vorinostat and romidepsin, were approved to treat cutaneous T cell lymphoma (17, 18). HDACis can induce high rates of apoptosis in many cell lines of hematological malignancy. The death receptor pathway and mitochondria/caspase pathway are both believed to be involved in HDACi-induced apoptosis (19). Such proapoptotic activity also leads to the investigation of HDACis in the inflammatory diseases (20). In this study, we examined the effects of VPA on EAE neuropathology. Oral or intraperitoneal administration of VPA reduced spinal cord inflammation, demyelination, and overall clinical symptoms of EAE. Mechanism study indicated that VPA induces apoptosis in activated T cells and maintains the immune homeostasis. This effect was found to be mainly mediated by the caspase-8/caspase-3 pathway. This phenomenon was also confirmed in T cells isolated from normal human subjects and MS patients. Our data suggest that VPA is a safe and effective therapy for MS.

MATERIALS AND METHODS

Human Samples—Human blood samples were obtained from patients of the outpatient clinic of Huashan Hospital (Shanghai, China) with clinically defined relapsing remitting MS and healthy volunteers from Tongji University. Informed consent was provided, and the sampling was completed in accordance with the guidelines of local institutional review boards.

Animals—Female C57BL/6 mice were purchased from Shanghai Laboratory Animal Center (Shanghai, China). All the mice were housed in the Tongji University animal care facility and were maintained in pathogen-free conditions. The mice were 8–9 weeks of age at the initiation of the experiment and were maintained on standard laboratory chow and water *ad libitum*. All of the experiments were approved and conducted in accordance with the guidelines of the Animal Care Committee of Tongji University.

Reagents—MOG_{35-55} (MEVGWYRSPFSRVVHLYRNGK) with a purity of >95% was purchased from GL Biochem (Shanghai, China). Complete Freund's adjuvant was purchased from Sigma-Aldrich. Percoll™ and Ficoll-Paque™ Plus were purchased from GE Healthcare. FITC anti-mouse CD45, FITC anti-mouse CD8a, phycoerythrin anti-mouse CD45R (B220), phycoerythrin Cy7 anti-mouse CD4, phycoerythrin anti-mouse IL17a, APC anti-mouse IFN-γ, and a BD Cytofix/Cytoperm™ kit were purchased from BD Biosciences. The Dynal® mouse CD4 cell negative isolation kit and Vybrant® apoptosis assay kit were from Invitrogen. APC anti-mouse CD4/CD8 and APC anti-human CD4/CD8 were purchased from Biolegend (San Diego, CA).

EAE Induction and Drug Treatment—Female C57BL/6 mice 8–9 weeks of age were immunized subcutaneously with 200 μg of MOG_{35-55} in complete Freund's adjuvant containing heat-killed *Mycobacterium tuberculosis* (H37Ra strain; 5 mg/ml; BD Diagnostics). Pertussis toxin (200 ng/mouse; Calbiochem) in PBS was administered intraperitoneally on days 0 and 2. The mice were examined daily for disease signs by researchers blinded to experimental conditions and were assigned scores on a scale of 0–5 as follows: 0, no clinical signs; 1, paralyzed tail; 2, paresis (weakness, incomplete paralysis of one or two hindlimbs); 3, paraplegia (complete paralysis of both hindlimbs); 4, paraplegia with forelimb weakness or paralysis; and 5, moribund state or death. For drug treatment, VPA was given via intraperitoneal injection (100–300 mg/kg of body weight) or oral administration (10–300 mg/kg of body weight) once daily from day 3 or 12 postimmunization until the end of the study. Water was given as vehicle control (100 μl/mouse).

Histopathological and Immunofluorescent Analysis—The mice were anesthetized and perfused with PBS (pH 7.4) followed by 4% (w/v) paraformaldehyde. Spinal cord samples were then fixed in 4% (w/v) paraformaldehyde overnight. Paraffin-embedded sections of spinal cord were stained with hematoxylin and eosin or with Luxol fast blue for analysis of inflammation or demyelination, respectively. Frozen sections of spinal cord were stained with anti-mouse CD45 or CD4 antibodies and then with appropriate fluorescent-labeled secondary antibodies.

Isolation and Analysis of CNS Leukocytes Infiltration—Spinal cords collected after PBS perfusion were homogenized in ice-cold tissue grinders and filtered through a 70-μm cell strainer, and the cells were collected by centrifugation at 500 × *g* for 10 min at 4 °C. The cells were resuspended in 8 ml of 37% Percoll and centrifuged onto 4 ml of 70% Percoll cushion in 15-ml tubes at 780 × *g* for 25 min at 25 °C. The cells at the 37–70% Percoll interface were collected and were subjected to flow cytometry analysis.

T Cell Proliferation—Naive mouse splenocytes were labeled with 10 mM carboxyfluorescein diacetate succinimidyl ester (CFSE) and then cultured for 48 h in complete RPMI 1640 medium containing 2 μg/ml anti-mouse CD3 antibody, 2 μg/ml anti-mouse CD28 antibody, and various concentrations VPA in 96-well plates. The CFSE fluorescence was determined by flow cytometry.

T Cell Apoptosis—Naive mouse splenocytes were cultured for 48 h in complete RPMI 1640 medium containing 10 ng/ml IL-2, 2 μg/ml anti-mouse CD3 antibody, and 2 μg/ml anti-mouse CD28 antibody in 48-well plates at a density of 3×10^6/well. Live cells were purified through the Ficoll ($\rho = 1.077$) density gradient and restimulated with anti-mouse CD3 (2 μg/ml) for 24, 48, or 72 h in the presence of various concentrations of VPA or the combination of VPA and the caspase inhibitor Z-VAD-FMK. Splenocytes isolated from naive or EAE mice at day 10 postimmunization were restimulated with MOG_{35-55} (20 μg/ml) for 24, 48, or 72 h in the presence of VPA (1 mM) or the combination of VPA (1 mM) and Z-VAD-FMK (10 μM). Human PBMC were isolated from whole blood samples by density gradient centrifugation on Ficoll-Paque. PBMC of healthy subjects were cultured in complete RPMI 1640 medium and restimulated with 2 μg/ml anti-human CD3 and 2 μg/ml anti-human CD28 antibodies in 48-well plates for 48 h. Live cells were purified through the Ficoll ($\rho = 1.077$) density gradient and restimulated with anti-human CD3 (2 μg/ml) for 24, 48, and 72 h in the presence of various concentrations of VPA or the combination of VPA and Z-VAD-FMK. PBMC of MS patients were cultured in complete RPMI 1640 and restimulated with MOG (20 μg/ml) for 24, 48, and 72 h in the presence

of VPA (1 mM) or the combination of VPA (1 mM) and Z-VAD-FMK (20 μM).

The cells were then stained with propidium iodide (PI) and annexin V in combination with anti-CD4 or anti-CD8 antibody. The percentage of apoptotic cells (annexin V positive and PI negative cells) was determined by flow cytometry.

$CD4^+$ T Cell Separation and in Vitro Differentiation—Naive $CD4^+$ T cells were prepared by magnetic cell separation (Invitrogen) from spleens of female C57BL/6 mice 8–9 weeks of age. The cells were activated with anti-mouse CD3 antibody (2 μg/ml) and anti-mouse CD28 antibody (2 μg/ml) and induced to differentiate into T_H-1 cells by supplementation with IL-12 (10 ng/ml) and anti-IL-4 (10 μg/ml). For T_H-17 differentiation, cells received anti-IL-4 (10 μg/ml), anti-IFN-γ (10 μg/ml), plus a T_H-17 mixture containing TGF-β1 (3 ng/ml), IL-6 (30 ng/ml), TNF-α (10 ng/ml), and IL-1β (10 ng/ml). VPA at various concentrations were added with the cytokine mixture, and the percentages of T_H-1 (IFN-γ^+) and T_H-17 (IL-17a$^+$) cells were analyzed with flow cytometry after 72 h of incubation.

To assess VPA-induced apoptosis in T_H-1 and T_H-17 cells, naive $CD4^+$ T cells were induced to differentiate into T_H-1 or T_H-17 for 72 h. Then the cells were cultured with fresh medium containing the cytokine mixture in the presence of VPA (1 mM) for another 48 h. The cells were then stained with annexin V in combination with anti-IFN-γ or anti-IL-17a antibody. The percentage of apoptotic cells (annexin V positive cells) was determined by flow cytometry.

Flow Cytometry—Splenocytes, PBMC, or CNS infiltrates were incubated for 5 h at 37 °C with phorbol 12-myristate 13-acetate (50 ng/ml; Sigma), ionomycin (750 ng/ml; Sigma), and brefeldin A (10 μg/ml; Sigma). Surface markers were stained with relevant antibodies. After surface staining, the cells were resuspended in fixation/permeabilization solution (Cytofix/Cytoperm kit; BD Pharmingen), and intracellular cytokine staining was done according to the manufacturer's protocol. Guava easyCyte™ 8HT system and GuavaSoft software were used for the analysis.

Real Time PCR—Total RNA were extracted from splenocytes using TRIzol reagent (Invitrogen) according to the manufacturer's instructions. The RNA was subjected to reverse transcription with random hexamer primer and Moloney murine leukemia virus reverse transcriptase (Promega). Real time PCR was conducted in the LightCycler quantitative PCR apparatus (Stratagene) using the SYBR Green JumpStart™ Taq ReadyMix™ kit (Sigma). Expression values were normalized to β-actin. The primer pairs used are as follows: caspase-1 sense, 5′-CCCCAGGCAAGCCAAAT-3′, antisense, 5′-GTGCCATCTTCTTTGTTCTGTTC-3′; caspase-3 sense, 5′-CTGACTGGAAAGCCGAAACTC-3′, antisense, 5′-TGGATGAACCACGACCCG-3′; caspase-6 sense, 5′-AGTACAAGATGGACCACAAGAGG-3′, antisense, 5′-GTTCTTCTGCTCTGAGGTCGTTA-3′; caspase-8 sense, 5′-GGAAGACATAACCCAACTCCG-3′, antisense, 5′-CTTGTCACCGTGGGATAGGAT-3′; caspase-9 sense, 5′-GATCAGGGGACATGCAGATATG-3′, antisense, 5′-TCTTGGCAGTCAGGTCGTTC-3′; and β-actin sense, 5′-GGCTGTATTCCCCTCCATCG-3′, antisense, 5′-CCAGTTGGTAACAATGCCATGTT-3′.

Western Blot—Splenocytes from EAE mice were washed once with PBS and lysed in lysis buffer by sonication for 30 s on ice. Protein concentration was determined by the BCA method (Thermo Scientific). The samples were loaded into 12% Tris/Gly gels, subjected to SDS-PAGE, and transferred onto a PVDF membrane (Millipore). Western blotting was performed using the rabbit anti-caspase-3 antibody and corresponding HRP-conjugated secondary antibody (Promega) and developed using Western Lightning Ultra extreme sensitivity kit (PerkinElmer Life Sciences).

Statistical Analysis—The results were expressed as the means ± S.E. The statistical significance of the EAE clinical scores between treatments were analyzed with two-way ANOVA test. The EAE scores at a given date were analyzed with a Mann-Whitney *U* test. Other analyses, including gene expression, cell percentage, and histological analysis, were assessed by Student's *t* test. $p < 0.05$ was considered statistically significant.

RESULTS

VPA Ameliorates Clinical Symptoms of EAE—To assess whether VPA has therapeutic effect in MS, EAE was induced in C57BL/6 mice by immunization with MOG_{35-55} peptide, and VPA was given once daily via intraperitoneal injection (Fig. 1*A*) or oral administration (Fig. 1*B*) from day 3 postimmunization until the end of the experiment. Water was given as vehicle control. VPA displayed dose-dependent inhibition of EAE severity in both series of experiments. Via intraperitoneal injection, VPA showed a better effect than oral administration at the same dosage; it not only significantly reduced the peak severity and cumulative clinical score of EAE, but also postponed the onset of the disease (Fig. 1, *A* and *B*). This is probably due to the higher initial blood concentration of VPA after intraperitoneal injection than the oral administration. Two low doses of VPA were also tested via oral administration. At 10 mg/kg, VPA had no effect in EAE mice (data not shown), but at 30 mg/kg, VPA displayed a slight but statistically significant beneficial effect in EAE mice (Fig. 1*B*). More interestingly, when given after the onset of the disease (day 12 postimmunization; Fig. 1*C*), VPA (300 mg/kg, orally) was still able to reduce the severity of EAE, which indicated the therapeutic benefit of this drug in addition to the preventative effect.

VPA Reduces CNS Leukocyte Infiltration and Neuropathy in EAE Mice—Histological examination of spinal cord was performed at day 17 postimmunization. Compared with vehicle treatment, VPA caused a dramatic decrease of leukocyte infiltration in the spinal cord (Fig. 1, *D* and *F*). Luxol fast blue staining also revealed less extensive demyelination in VPA-treated EAE mice compared with the vehicle control group (Fig. 1, *E* and *G*). The CNS leukocyte infiltration was further analyzed by *in situ* immunofluorescent staining of the spinal cord sections. Consistent with the results of hematoxylin and eosin staining, VPA treatment reduced the number of $CD45^+$ and $CD4^+$ T cells (Fig. 2*A*) in the spinal cord sections of EAE mice.

The CNS leukocyte infiltration was also quantified by flow cytometry analysis at day 17 postimmunization. The results again confirmed that both the $CD45^+$ infiltrates (Fig. 2, *B*, *top*

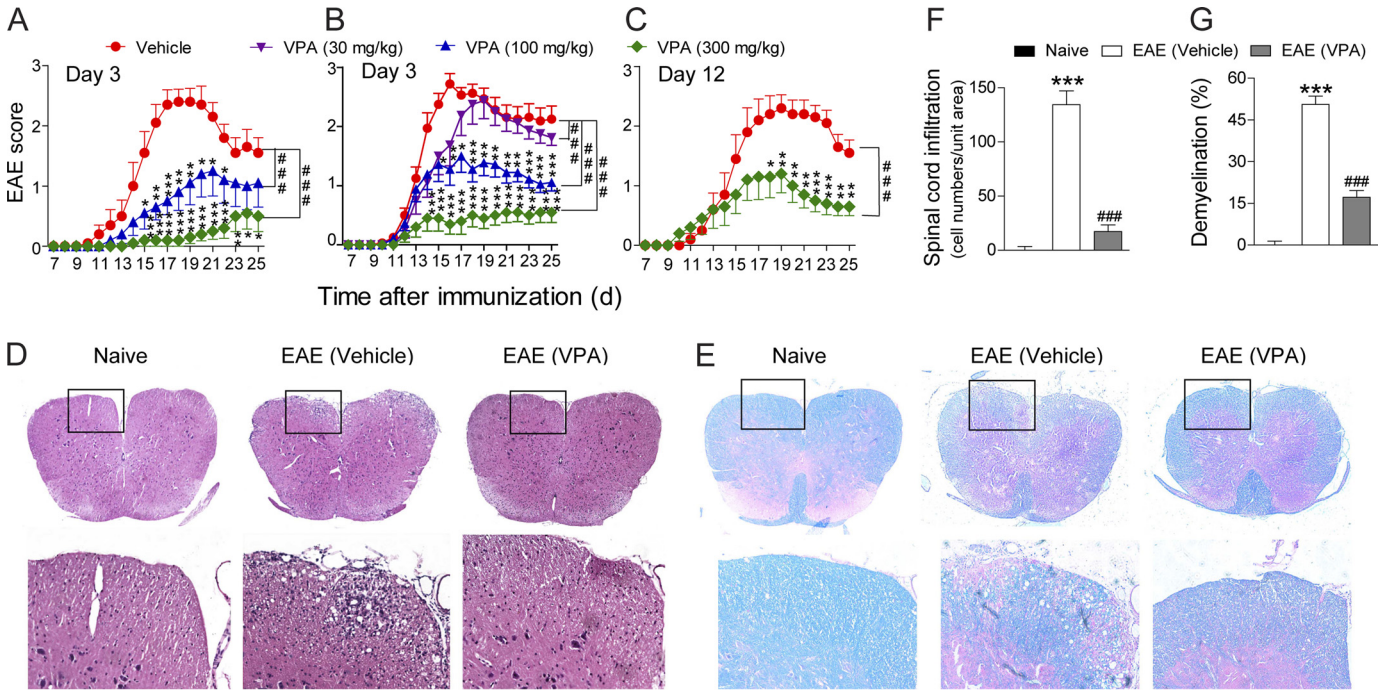

FIGURE 1. **VPA alleviates clinical symptoms of EAE.** *A–C*, EAE was induced in female C57/B6 mice by immunization with MOG_{35-55}. VPA was given once daily starting from day 3 postimmunization via intraperitoneal injection (*A*) or oral administration (*B*) or starting from day 12 by oral administration (*C*) until the end of the experiment, and clinical scores were recorded every day. Control groups were given oral or intraperitoneal injection of saline. The data represent the means ± S.E. ($n = 10$). ###, $p < 0.001$ (two-way ANOVA test). *, $p < 0.05$; **, $p < 0.01$; ***, $p < 0.001$ *versus* vehicle control (Mann-Whitney *U* test). *D* and *E*, hematoxylin and eosin staining (*D*) and Luxol fast blue staining (*E*) of paraffin sections of spinal cords isolated from naive, vehicle, or VPA-treated (300 mg/kg, orally, starting from day 3) EAE mice on day 17 after immunization. The *boxed areas* in the *top rows* are presented enlarged in the *bottom row*. *F* and *G*, number of CNS infiltrates in the hematoxylin- and eosin-stained sections and the area of demyelination in the Luxol fast blue stained sections are quantified. Four animals from each group were sacrificed, and 15 sections of the spinal cord of each animal were analyzed. ***, $p < 0.001$, *versus* naive control; ###, $p < 0.001$, *versus* vehicle control (Student's *t* test).

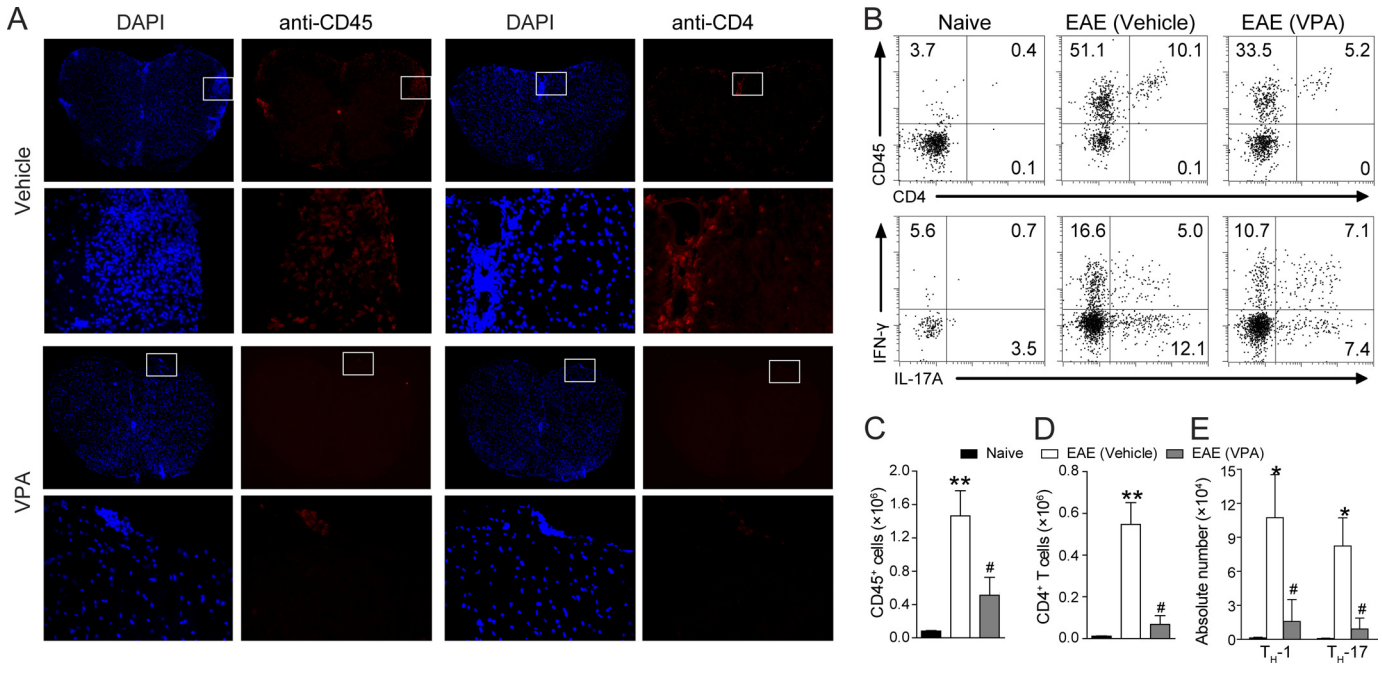

FIGURE 2. **VPA reduces CNS infiltration of pathogenic T cells.** *A*, frozen sections were prepared from spinal cords isolated from vehicle or VPA-treated EAE mice at day 17 postimmunization, and $CD45^+$ cells and $CD4^+$ T cells were visualized with antibody staining. DAPI was used to stain the nuclei. For three mice/group, six serial sections were stained, and representative sections are presented. The *boxed areas* in the *first* and *third rows* are presented enlarged in the *second* and *fourth rows*, respectively. *B–E*, CNS infiltrates were isolated with 37/70% Percoll from naive and MOG-EAE mice treated with vehicle or VPA (300 mg/kg, orally, starting from day 3) at day 17 postimmunization and the number of $CD45^+$ infiltrates (*B*, *top panel*, and *C*), $CD4^+$ T cells (*B*, *top panel*, and *D*), and T_H-1 and T_H-17 cells (*B*, *bottom panel*, and *E*) were analyzed by flow cytometry. The data represent the means ± S.E. ($n = 6$). *, $p < 0.05$; **, $p < 0.01$ *versus* naive control; #, $p < 0.05$, *versus* vehicle control (Student's *t* test).

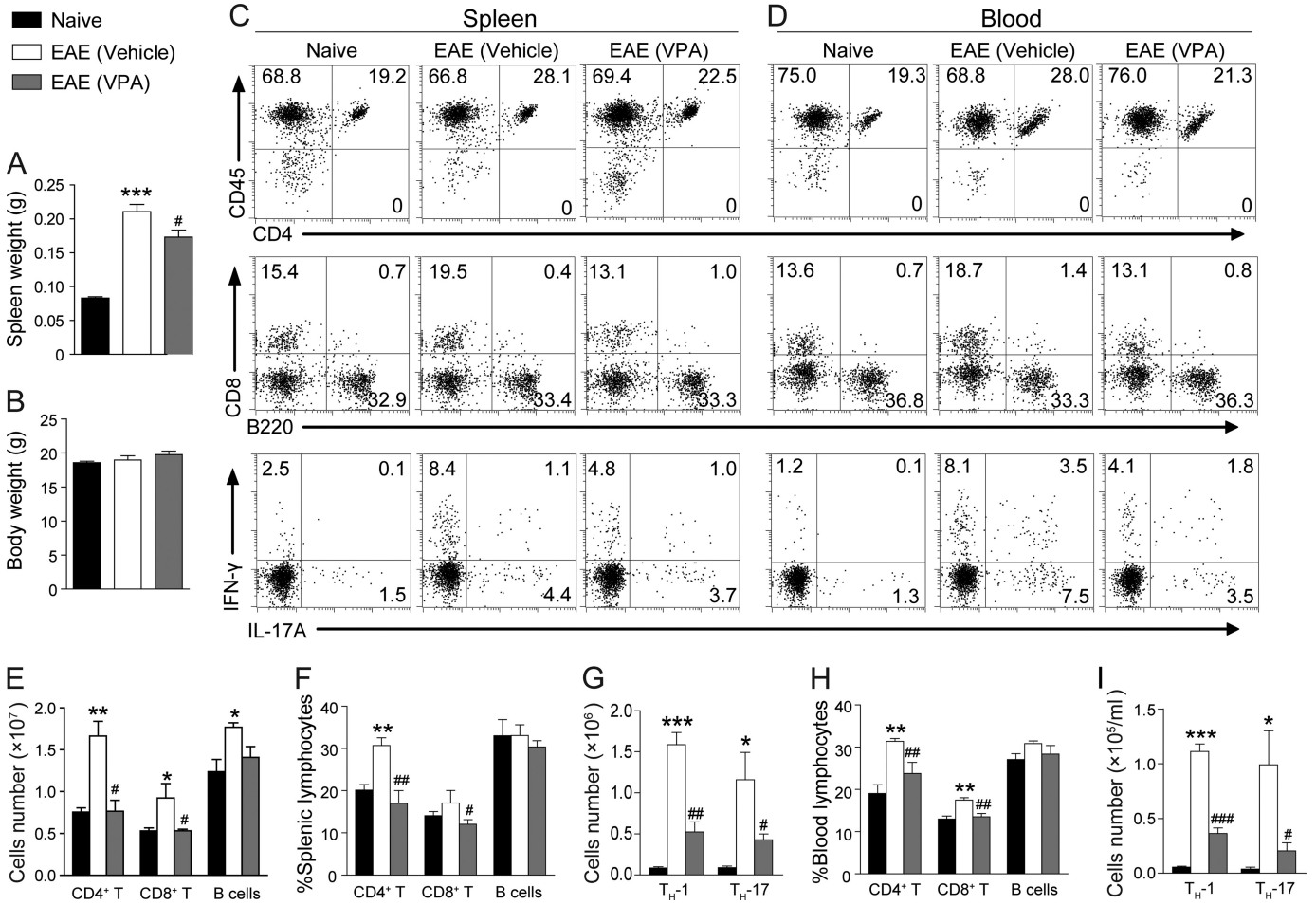

FIGURE 3. **VPA reduces periphery T cell population in EAE mice.** *A* and *B*, naive and EAE mice were treated with VPA (300 mg/kg, orally, starting from day 3) or vehicle. The body weight (*B*) and spleen weight (*A*) were measured at day 10. The data are the means ± S.E. ($n = 6$). ***, $p < 0.001$, *versus* naive control; #, $p < 0.05$, *versus* vehicle control (Student's *t* test). *C* and *D*, leukocytes were isolated from the spleen (*C*) and circulating blood (*D*) of naive and EAE animals treated with VPA (300 mg/kg, orally, starting from day 3) or vehicle control at day 10 postimmunization, and the percentage and number of $CD4^+$ T cells, $CD8^+$ T cells, and B cells ($B220^+$) were analyzed with surface staining and flow cytometry. T_H-1 and T_H-17 cells were analyzed by intracellular staining of IFN-γ and IL-17a in the CD4 gate. *E–G*, statistical analysis of *C*. *H* and *I*, statistical analysis of *D*. The data represent the means ± S.E. ($n = 6$). *, $p < 0.05$; **, $p < 0.01$; ***, $p < 0.001$ *versus* naive control. #, $p < 0.05$; ##, $p < 0.01$; ###, $p < 0.001$ *versus* vehicle treatment group (Student's *t* test).

row, and *C*) and $CD4^+$ T cells (Fig. 2, *B*, *top row*, and *D*) accumulated in the CNS of EAE mice were decreased after VPA treatment. The IL-17 producing T_H-17 cells and the IFN-γ producing T_H-1 cells are the major pathogenic T effector cells in EAE. Therefore we quantified the number of T_H-1 and T_H-17 cells in the CNS infiltrates. After VPA treatment, the absolute number of both T_H-17 and T_H-1 cells were significantly decreased (Fig. 2, *B*, *bottom row*, and *E*). Taken together, these data indicate that VPA treatment significantly reduces EAE severity accompanied by decreased CNS inflammation and demyelination.

VPA Reduces Peripheral $CD4^+$ and $CD8^+$ T Cells in EAE Mice—Expansion and differentiation of $CD4^+$ T cells is believed to be a prerequisite of EAE pathogenesis (21). At day 10 postimmunization, we observed that the spleen of the EAE mice were significantly larger than the naive controls even before the onset of the clinical symptoms, VPA treatment significantly reduced the size of the spleen in EAE animals without affecting the whole body weight (Fig. 3, *A* and *B*). The body weight of EAE mice usually drops quickly after the onset of the disease, but at day 10, there is no difference of body weight between the naive and EAE animals (Fig. 3*B*).

Surface staining of proper markers showed that the percentage and number of $CD4^+$ T cells were dramatically increased in EAE mice, whereas VPA treatment significantly reduced the percentage and the number of $CD4^+$ T cells and $CD8^+$ T cells in the spleen. After EAE induction, the number of B cells in the spleen did increase, although the increase was not as dramatic as T cells. So percent-wise, the frequency of B cells in the spleen was not changed, and VPA did not significantly affect the B cells population (Fig. 3, *C*, *top two rows*, *E*, and *F*). With intracellular cytokine staining, we found that the number of T_H-1 and T_H-17 cells in the $CD4^+$ population was significantly reduced in the spleen of VPA-treated EAE mice (Fig. 3, *C*, *bottom row*, and *G*). Similar results were obtained in the peripheral blood samples (Fig. 3, *D*, *H*, and *I*).

VPA Blocks Proliferation and Induces Apoptosis in Activated T Cells—Our results showed that the frequency of T cells was greatly reduced in the periphery immune tissues upon VPA treatment. Based on these observations, we speculated that

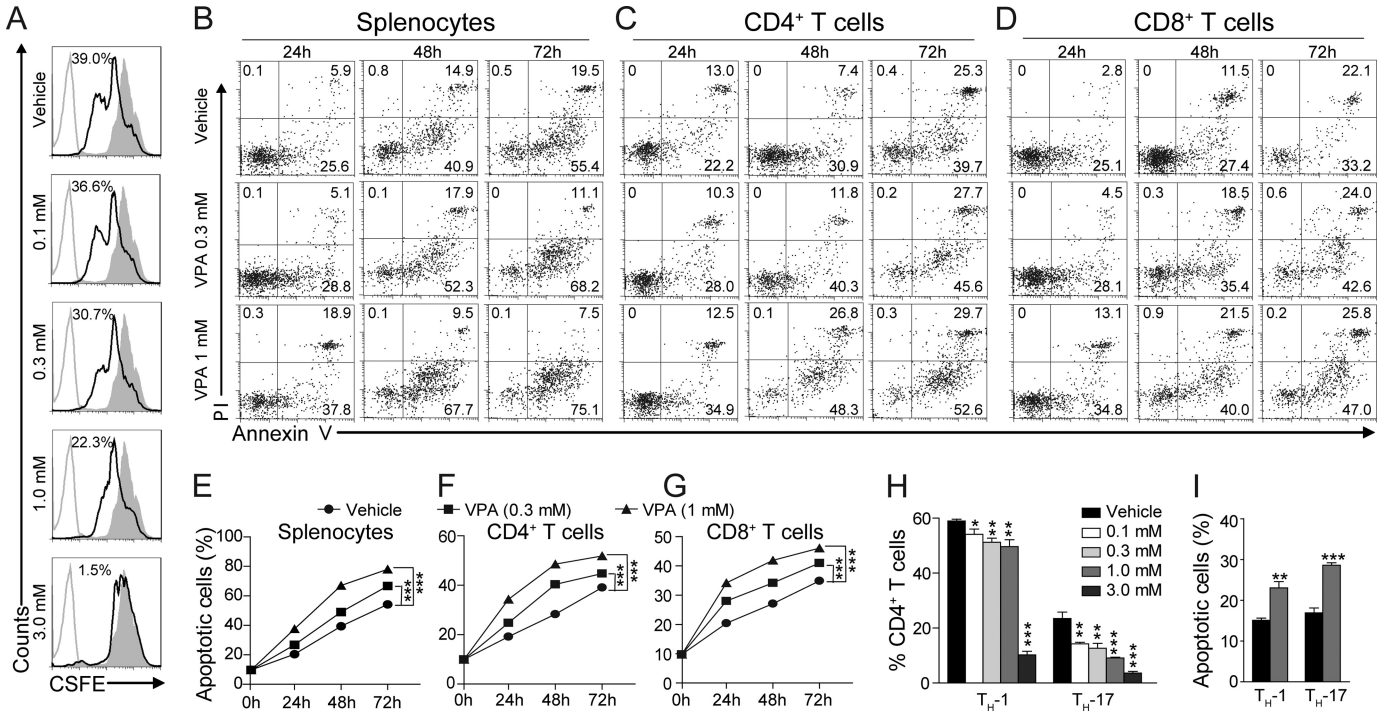

FIGURE 4. **VPA blocks proliferation and induces apoptosis in activated T cells.** *A*, naive mouse splenocytes were stimulated with 2 μg/ml anti-mouse CD3 and 2 μg/ml anti-mouse CD28 in the presence of VPA; cell proliferation was assessed with CFSE staining. *B–D*, representative FACS plots of apoptosis (annexin V positive and PI negative) in total splenocytes (*B*), CD4$^+$ (*C*), or CD8$^+$ (*D*) T cells treated with VPA. *E–G*, statistical analysis of apoptosis presented in *B–D*. The data are from three independent experiments (means $\pm$ S.E.). ***, $p < 0.001$, *versus* vehicle control (two-way ANOVA). *H*, naive CD4$^+$ T cells were induced to differentiate into T_H-1 or T_H-17 cells in the presence of VPA. *I*, apoptosis of T_H-1 and T_H-17 cells induced by VPA (1 mM). The data are the means $\pm$ S.E. of three independent experiments. *, $p < 0.05$; **, $p < 0.01$; ***, $p < 0.001$ *versus* vehicle control (Student's *t* test).

VPA might influence the proliferation, survival, or apoptosis of T cells. Splenocytes isolated from naive mice were activated with anti-mouse CD3 and anti-mouse CD28 in the presence of VPA for 48 h. The proliferation of T cells *in vitro* was determined by the CFSE method. As shown in Fig. 4*A*, VPA dose-dependently suppressed the T cell antigen-stimulated cell proliferation.

Next, early apoptosis in splenocytes and subpopulations was measured with annexin V (positive) and PI (negative) staining after the treatment of VPA (0.3 and 1 mM) for various durations (24–72 h). Activated splenocytes underwent apoptosis in a time-dependent fashion (Fig. 4, *B* and *E*) as previously reported (14, 22). VPA enhanced apoptosis in splenocytes in a dose-dependent way (Fig. 4, *B* and *E*). Subpopulation analysis with cell surface markers revealed that VPA enhanced apoptosis in both the CD4$^+$ and CD8$^+$ T cells after activation *in vitro* (Fig. 4, *C*, *D*, *F*, and *G*).

Considering that T_H-17 and T_H-1 cells are the major pathogenic T effector cells in EAE, we tested whether VPA affect their differentiation and apoptosis *in vitro*. Naive CD4$^+$ T cells were induced to differentiate into T_H-1 or T_H-17 cells by supplementation with differentiation factors in the presence of VPA. The cells were harvested 72 h later, and intracellular staining for IFN-γ or IL-17a was performed. Upon FACS analysis, VPA was found to significantly block the differentiation of both the T_H-1 and T_H-17 cells *in vitro* (Fig. 4*H*), and T_H-17 differentiation seems more susceptible to VPA treatment. To assess the apoptosis-inducing effect of VPA in T_H-1 and T_H-17 cells, naive CD4$^+$ T cells were allowed to differentiate into T_H-1 or T_H-17 cells for 72 h, and then VPA (1 mM) was added for another 48 h. VPA significantly increased the percentage of apoptotic cells in both T_H-1 (IFN-γ^+) and T_H-17 (IL-17a$^+$) populations (Fig. 4*I*).

VPA Induces T Cell Apoptosis via Caspase Pathway—Caspase-dependent cascade is one of the major pathways that regulate cell apoptosis (23). We found the mRNA levels of caspase-3 and 8 in the splenocytes isolated from EAE mice treated with VPA were significantly up-regulated compared with the vehicle-treated ones (Fig. 5*A*). More interestingly, the mRNA levels of caspases-3, -8, and -9 were only found to be significantly up-regulated in the T cell population after VPA treatment (Fig. 5, *B* and *C*). Caspases are cysteine proteases critically involved in apoptosis. The caspases convey the apoptotic signal in a proteolytic cascade, with the upstream caspases (such as caspase-8 and -9) cleaving and activating the downstream ones, such as caspase-3, which lead to apoptosis by direct degradation of cellular targets (24). We then measured the protein level of caspase-3 in the splenocytes from EAE mice treated with VPA or vehicle. In the VPA-treated group, the acetylation level of H3 was significantly increased. The protein levels of both the pro-caspase-3 and cleaved caspase-3 (active form) were also significantly higher in the VPA treatment group (Fig. 5, *D* and *E*).

Next we tested the effect of VPA on MOG-specific T cells. Splenocytes were isolated from naive or EAE mice at day 10 postimmunization and reactivated with MOG (20 μg/ml) *in vitro* in the presence of VPA (1 mM) or the combination of VPA and the pan-caspase inhibitor Z-VAD-FMK (10 μM) (25), and

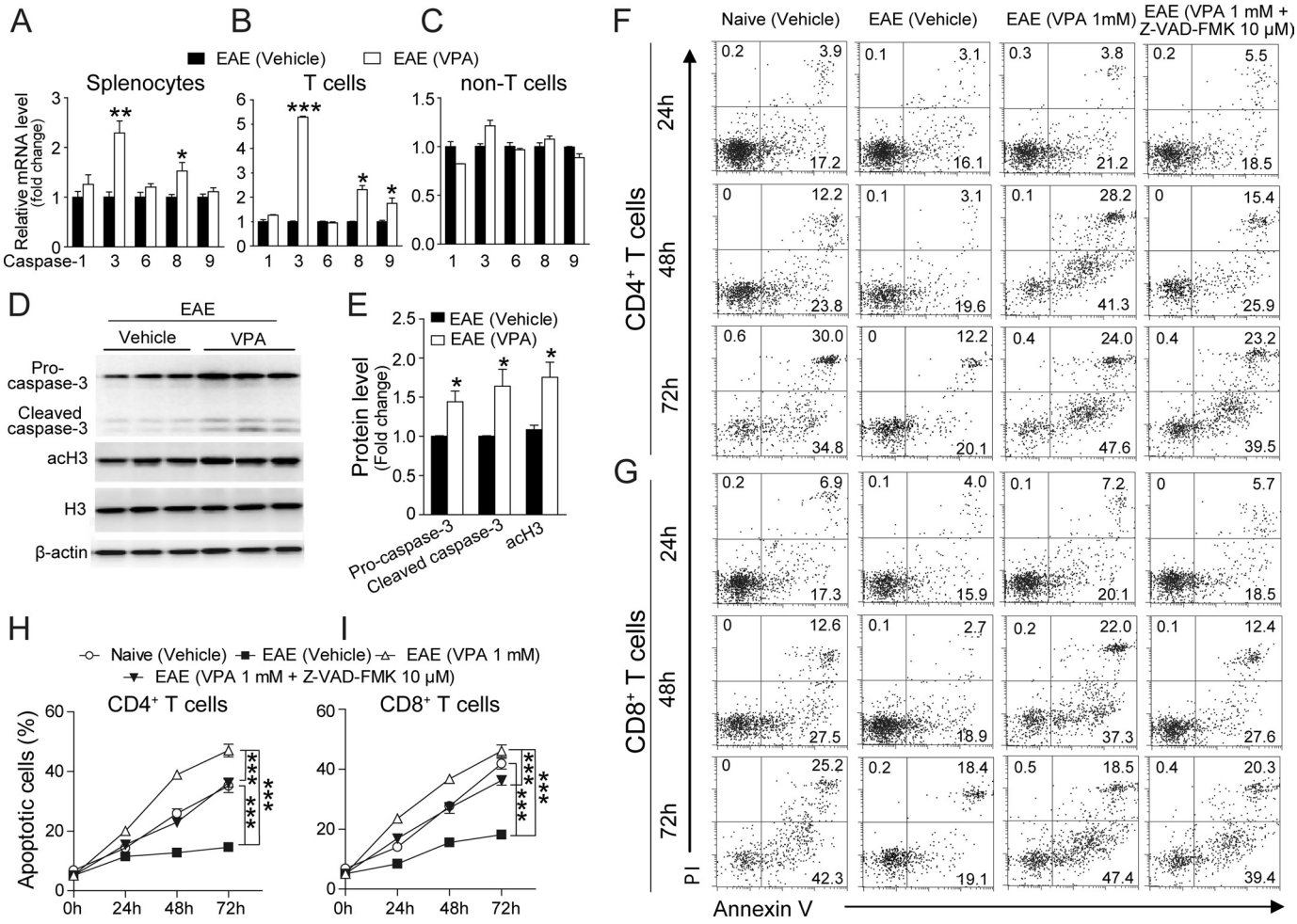

FIGURE 5. **VPA induces T cell apoptosis via caspase pathway.** *A–C*, total splenocytes (*A*), T cells (*B*), and non-T cells (*C*) were isolated from EAE mice treated with VPA (300 mg/kg, orally, starting from day 3) or vehicle at day 10 postimmunization, and the expression levels of caspases-1, -3, -6, -8, and -9 were analyzed with quantitative PCR. The data represent the means ± S.E. ($n = 6$). *, $p < 0.05$; **, $p < 0.01$; ***, $p < 0.001$ *versus* vehicle control (Student's *t* test). *D*, splenocytes were isolated from EAE mice treated with VPA (300 mg/kg, orally, starting from day 3) or vehicle at day 10 postimmunization, and the protein levels of pro-caspase-3, cleaved (activated) caspase-3, and acetylated histone H3 were analyzed with Western blot. The image presented is representative of three independent experiments, and three mice from each group were analyzed. *E*, statistical analysis of the protein levels presented in *D*. The data are the means ± S.E. *, $p < 0.05$ *versus* vehicle control (Student's *t* test). *F* and *G*, representative FACS plots of apoptosis in MOG specific $CD4^+$ (*F*) or $CD8^+$ (*G*) T cells isolated from naive and EAE mice at day 10 treated with VPA (1 mM) or the combination of VPA (1 mM) and Z-VAD-FMK (10 μM). *H* and *I*, statistical analysis of *F* and *G*. The data are from three independent experiments, each performed in triplicate (means ± S.E.). ***, $p < 0.001$ (two-way ANOVA).

apoptosis in the $CD4^+$ and $CD8^+$ T subpopulations were measured with FACS (Fig. 5, *F* and *G*). T cells from naive animals displayed a moderate level of apoptosis (Fig. 5, *H* and *I*, *open circles*), whereas the T cells from EAE mice showed very low levels of apoptosis (*closed squares*). VPA treatment greatly promoted apoptosis in both MOG specificity $CD4^+$ and $CD8^+$ T cells (*open triangles*), and such an effect was significantly inhibited by Z-VAD-FMK (*closed triangles*). Taken together, these data indicate that VPA induces T cell apoptosis via the caspase pathway.

VPA Promotes Human T Cell Apoptosis—It would be interesting to know whether the apoptosis-inducing effect of VPA in mouse T cells could also be applied to human T cells. Human PBMCs were isolated from healthy subjects and stimulated with anti-human CD3 and anti-human CD28 in the presence of VPA (0.3 or 1 mM) or the combination of VPA (1 mM) and Z-VAD-FMK (20 μM), and the apoptosis in the $CD4^+$ and $CD8^+$ T subpopulations was measured with FACS (Fig. 6, *A* and *B*). As observed in mouse T cells, VPA dose-dependently enhanced apoptosis in normal human $CD4^+$ and $CD8^+$ T cells *in vitro* (Fig. 6, *C* and *D*), and the effect of VPA was significantly inhibited by the pan-caspase inhibitor, Z-VAD-FMK (Fig. 6, *E* and *F*).

Next, we tested VPA on the PBMCs isolated from three MS patients (Table 1). These cells were stimulated with MOG (20 μg/ml) in the presence of VPA (1 mM) or the combination of VPA (1 mM) and Z-VAD-FMK (20 μM). Compared with the T cells from the healthy subjects, the cells isolated from the MS patients showed minimal apoptosis in the first 48 h of *in vitro* culture (Fig. 7). VPA enhanced the apoptosis of both $CD4^+$ and $CD8^+$ T cells isolated from MS patients (Fig. 7) to a level similar to that of the spontaneous apoptosis observed in T cells isolated from healthy subjects (Fig. 6). This effect was significantly inhibited by Z-VAD-FMK (Fig. 7). These data indicate that VPA also induces apoptosis in human T cells via the caspase pathway.

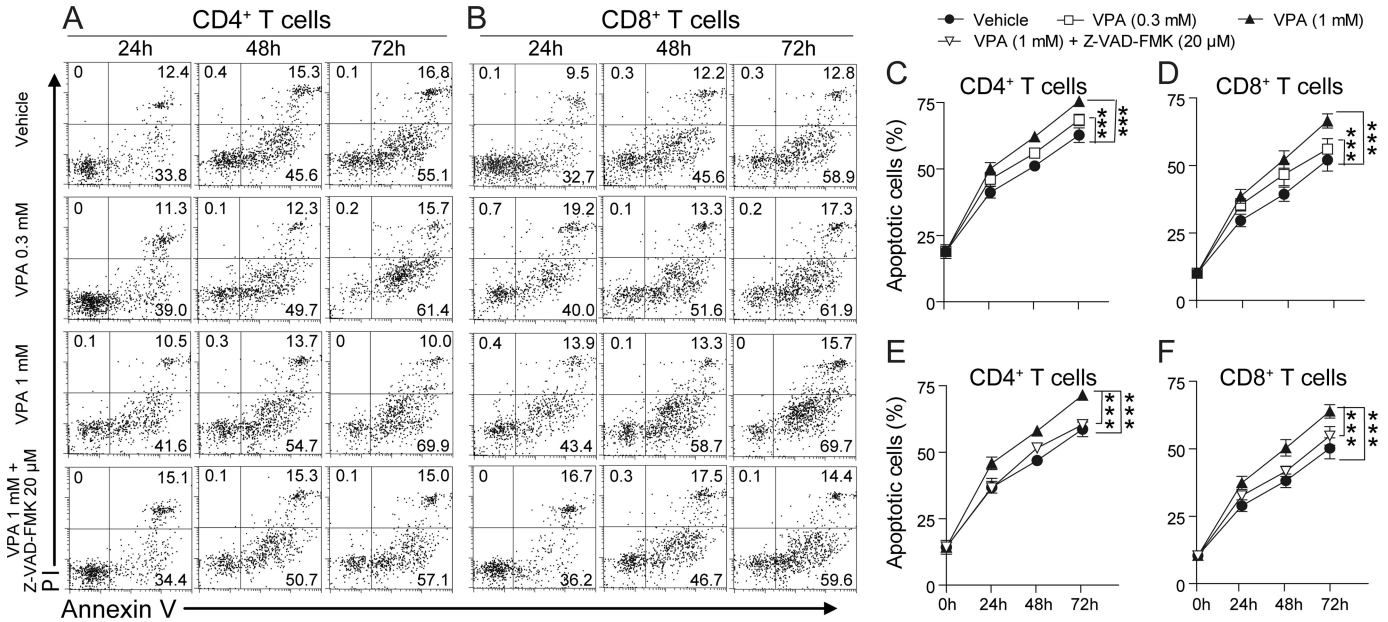

FIGURE 6. **VPA promotes apoptosis in T cells from healthy human.** *A* and *B*, representative FACS plots of apoptosis (annexin V positive and PI negative) in healthy human $CD4^+$ (*A*) or $CD8^+$ (*B*) T cells treated with VPA (0.3 mM and 1 mM) or the combination of VPA (1 mM) and Z-VAD-FMK (20 μM) for 24, 48, or 72 h. *C* and *D*, statistical analysis of VPA-induced apoptosis in $CD4^+$ or $CD8^+$ T cells presented in the *top three rows* in *A* and *B*. *E* and *F*, statistical analysis of the effect of Z-VAD-FMK on VPA-induced apoptosis presented in the *bottom row* in *A* and *B*. The data are from three independent experiments (means ± S.E.). ***, $p <$ 0.001 (two-way ANOVA).

TABLE 1

Characteristics of patients

Sample size is the total number of subjects. Age is presented in years ±S.E. Sex is presented as the total number (with percentage of group in parentheses). The expanded Disability Status Scale (EDSS) score is presented as the mean ± S.E.

	Relapsing Remitting MS
Sample size	3
Age	46.7 ± 5.0
Sex	
Female	2 (67%)
Male	1 (33%)
EDSS score	1.7 ± 0.3

DISCUSSION

Disregulation of cell survival and death can cause many diseases, including cancer and autoimmune diseases. Inducing cell apoptosis, a major strategy used in cancer therapy, might also be useful in treating autoimmune disorders. In recent years, many efforts have been made to develop HDACis as a cancer treatment (26, 27). Currently, two HDACis, vorinostat and romidepsin, are approved to treat cutaneous T cell lymphoma (17, 18), and a number of HDACis are at various stages of clinical study. Among them, VPA, the well known anti-psychotic drug, is under clinical investigation to treat breast cancer, ovarian cancer, various form of leukemia, and many other malignancies (listed on the National Institutes of Health Clinical Trials website). The exact mechanisms by which these compounds may work are still unclear, but epigenetic pathways that eventually lead to cell growth arrest, differentiation, or apoptosis have been proposed (29). Such epigenetic modulatory and pro-apoptotic activity also lead to the investigation of HDACis in the inflammatory diseases (20).

Herein, we demonstrated that VPA effectively reduces EAE severity accompanied by decreased CNS inflammation and demyelination, and the induction of apoptosis in autoreactive T cells might be one of the mechanisms by which VPA exerts its therapeutic effect. Peripheral $CD4^+$ T cells are maintained in a homeostatic balance between their production and elimination (30). Upon antigen stimulation, naive $CD4^+$ T cells proliferate and differentiate into effector T cells to regulate immune responses. Then several distinct mechanisms, including cell inactivation, activation-induced cell death, and activated T cell-autonomous death, will lead to the reduction in the number and activity of effector T cells and thus the immune responses. Failure of $CD4^+$ T cell death may prolong the immune responses and result in disturbed T cell homeostasis and autoimmune diseases including MS (2). Recently, $CD8^+$ T cells are also implicated in the pathogenesis of EAE. The $CD8^+$ T lymphocytes detected in MS lesions demonstrate characteristics of activated and clonally expanded cells, supporting the notion that these cells actively contribute to the observed injury (7). Our results demonstrated that VPA enhances apoptosis in anti-CD3/CD28 activated or MOG-restimulated $CD4^+$ and $CD8^+$ T cells, but not in B cell population, indicating that the main effect of VPA is to restore T cell homeostasis in EAE mice.

Two major pathways have been implicated in regulating the death of T cells. One is the mitochondria-mediated pathway modulated by the Bcl-2 protein family, which is composed of pro- and antiapoptotic members. In Bcl-2-deficient mice, T cells are more susceptible to death (31, 32), whereas in *Bcl2*-transgenic mice, lymphocytes are more resistant to apoptotic stimuli, and autoimmune symptoms have been reported (33). The other pathway is through the activation of caspase cascade (34, 35), which is typically induced by cell surface receptors such as TNF, TRAIL receptors, and Fas, which are death factors for activated $CD4^+$ T cells. In our study, VPA was found to significantly and specifically enhance the mRNA expression of

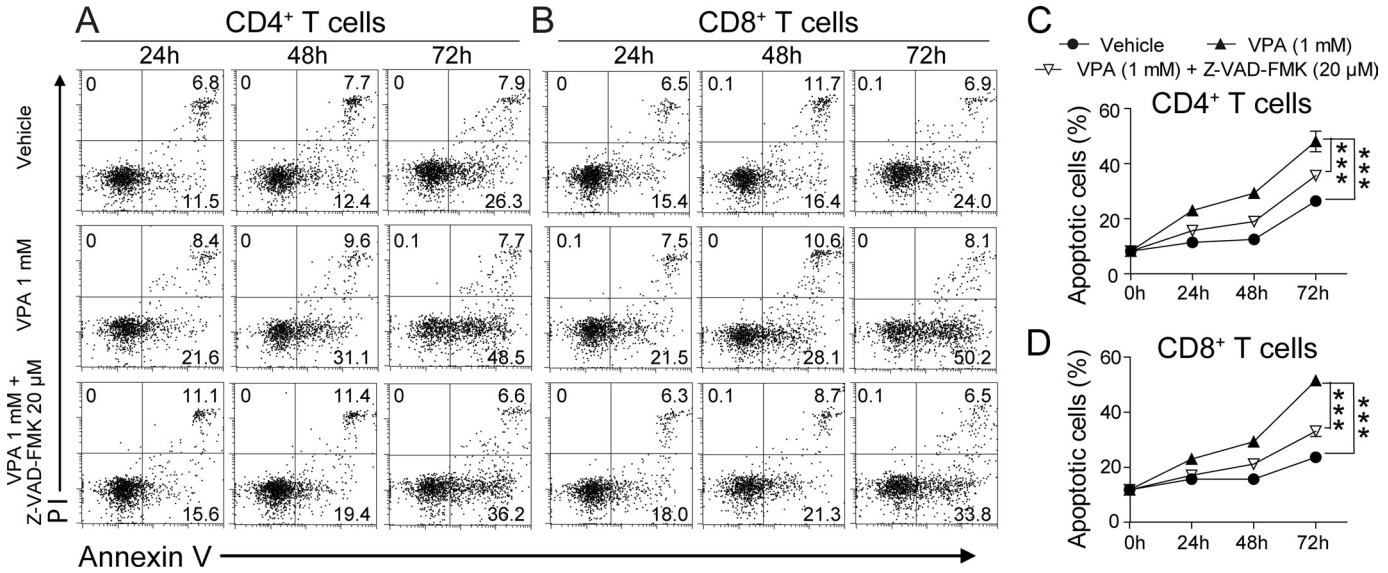

FIGURE 7. **VPA promotes apoptosis in T cells from MS patients.** *A* and *B*, representative FACS plots of apoptosis (annexin V positive and PI negative) in MS patient $CD4^+$ (*A*) or $CD8^+$ (*B*) T cells treated with VPA (1 mM) or the combination of VPA (1 mM) and Z-VAD-FMK (20 μM) for 24, 48, or 72 h. *C* and *D*, statistical analysis of *A* and *B*. The data are from three independent experiments (means ± S.E.). ***, $p < 0.001$ (two-way ANOVA).

caspases-3, -8, and -9 in T cells. Caspase-3 is a downstream caspase that is cleaved and activated by upstream caspases such as caspase-8 and 9 and that leads to apoptosis by direct degradation of cellular targets (24). We found the protein levels of both the pro-caspase-3 and cleaved caspase-3 (active form) were also significantly higher in the splenocytes of VPA-treated mice. The fact that the pan-caspase inhibitor Z-VAD-FMK effectively blocked VPA-induced apoptosis in T cells further confirmed our hypothesis that VPA enhances T cell death via the caspase pathway.

Other mechanisms have also been proposed to underlie the beneficial effects of HDACis in autoimmunity. IL-2 is a cytokine essential for immune responses and T cell homeostasis (36). HDACi trichostatin A and FR235222 have been shown to inhibit *IL-2* gene expression and to possess immunosuppressive activity *in vivo* (37, 38). Trichostatin A has also been shown to up-regulate antioxidant, anti-excitotoxicity, and pro-neuronal growth and differentiation mRNAs and protect neurons from apoptosis in EAE (4). VPA has been reported to remarkably attenuate MCAO-induced blood-brain barrier disruption and brain edema via HDAC inhibition-mediated suppression of NF-κB activation, MMP-9 induction, and tight junction degradation (39).

With their combined neuroprotective, neurotrophic, and anti-inflammatory effects, HDACis are emerging as a new strategy to treat neurodegenerative disorders (28). VPA, with its long history of clinical use in psychiatry and neurology and our new evidence to maintain immune cell homeostasis, might be repositioned as a promising new treatment for MS.

REFERENCES

1. Van Parijs, L., and Abbas, A. K. (1998) Homeostasis and self-tolerance in the immune system. Turning lymphocytes off. *Science* **280,** 243–248
2. Sun, H., Gong, S., Carmody, R. J., Hilliard, A., Li, L., Sun, J., Kong, L., Xu, L., Hilliard, B., Hu, S., Shen, H., Yang, X., and Chen, Y. H. (2008) TIPE2, a negative regulator of innate and adaptive immunity that maintains immune homeostasis. *Cell* **133,** 415–426
3. Massacesi, L. (2002) Compartmentalization of the immune response in the central nervous system and natural history of multiple sclerosis. Implications for therapy. *Clin. Neurol. Neurosurg.* **104,** 177–181
4. Camelo, S., Iglesias, A. H., Hwang, D., Due, B., Ryu, H., Smith, K., Gray, S. G., Imitola, J., Duran, G., Assaf, B., Langley, B., Khoury, S. J., Stephanopoulos, G., De Girolami, U., Ratan, R. R., Ferrante, R. J., and Dangond, F. (2005) Transcriptional therapy with the histone deacetylase inhibitor trichostatin A ameliorates experimental autoimmune encephalomyelitis. *J. Neuroimmunol.* **164,** 10–21
5. Jäger, A., Dardalhon, V., Sobel, R. A., Bettelli, E., and Kuchroo, V. K. (2009) Th1, Th17, and Th9 effector cells induce experimental autoimmune encephalomyelitis with different pathological phenotypes. *J. Immunol.* **183,** 7169–7177
6. York, N. R., Mendoza, J. P., Ortega, S. B., Benagh, A., Tyler, A. F., Firan, M., and Karandikar, N. J. (2010) Immune regulatory CNS-reactive CD8+T cells in experimental autoimmune encephalomyelitis. *J. Autoimmun.* **35,** 33–44
7. Mars, L. T., Saikali, P., Liblau, R. S., and Arbour, N. (2011) Contribution of CD8 T lymphocytes to the immuno-pathogenesis of multiple sclerosis and its animal models. *Biochim. Biophys. Acta* **1812,** 151–161
8. Wahl, S. M., Wen, J., and Moutsopoulos, N. (2006) TGF-β. A mobile purveyor of immune privilege. *Immunol. Rev.* **213,** 213–227
9. Anderson, A. C., Reddy, J., Nazareno, R., Sobel, R. A., Nicholson, L. B., and Kuchroo, V. K. (2004) IL-10 plays an important role in the homeostatic regulation of the autoreactive repertoire in naive mice. *J. Immunol.* **173,** 828–834
10. Fan, H. C., Ren, X. R., Yu, J. Z., Guo, M. F., Ji, N., Sun, Y. S., Liang, L. Y., and Ma, C. G. (2009) [Suppression of murine EAE by triptolide is related to downregulation of INF-gamma and upregulation of IL-10 secretion in splenic lymphocytes]. *Xi Bao Yu Fen Zi Mian Yi Xue Za Zhi* **25,** 222–225
11. Huss, D. J., Winger, R. C., Cox, G. M., Guerau-de-Arellano, M., Yang, Y., Racke, M. K., and Lovett-Racke, A. E. (2011) TGF-β signaling via Smad4 drives IL-10 production in effector Th1 cells and reduces T-cell trafficking in EAE. *Eur. J. Immunol.* **41,** 2987–2996
12. Brunner, T., Wasem, C., Torgler, R., Cima, I., Jakob, S., and Corazza, N. (2003) Fas (CD95/Apo-1) ligand regulation in T cell homeostasis, cell-mediated cytotoxicity and immune pathology. *Semin. Immunol.* **15,** 167–176
13. Saint Fleur, S., Hoshino, A., Kondo, K., Egawa, T., and Fujii, H. (2009) Regulation of Fas-mediated immune homeostasis by an activation-induced protein, Cyclon. *Blood* **114,** 1355–1365
14. Shi, Y., Feng, Y., Kang, J., Liu, C., Li, Z., Li, D., Cao, W., Qiu, J., Guo, Z., Bi,

E., Zang, L., Lu, C., Zhang, J. Z., and Pei, G. (2007) Critical regulation of CD4+ T cell survival and autoimmunity by β-arrestin 1. *Nat. Immunol.* **8,** 817–824
15. Amano, R., Mizukawa, M., Ohtsuka, Y., and Ohtahara, S. (1990) High-dose sodium valproate therapy for childhood refractory epilepsy. *Jpn J. Psychiatry Neurol.* **44,** 343–344
16. Guerrini, R. (2006) Valproate as a mainstay of therapy for pediatric epilepsy. *Paediatr. Drugs* **8,** 113–129
17. Mann, B. S., Johnson, J. R., Cohen, M. H., Justice, R., and Pazdur, R. (2007) FDA approval summary. Vorinostat for treatment of advanced primary cutaneous T-cell lymphoma. *Oncologist* **12,** 1247–1252
18. Campas-Moya, C. (2009) Romidepsin for the treatment of cutaneous T-cell lymphoma. *Drugs Today* **45,** 787–795
19. Dickinson, M., Johnstone, R. W., and Prince, H. M. (2010) Histone deacetylase inhibitors. Potential targets responsible for their anti-cancer effect. *Invest. New Drugs.* **28,** S3–S20
20. Adcock, I. M. (2007) HDAC inhibitors as anti-inflammatory agents. *Br. J. Pharmacol.* **150,** 829–831
21. Sonobe, Y., Jin, S., Wang, J., Kawanokuchi, J., Takeuchi, H., Mizuno, T., and Suzumura, A. (2007) Chronological changes of $CD4^+$ and $CD8^+$ T cell subsets in the experimental autoimmune encephalomyelitis, a mouse model of multiple sclerosis. *Tohoku J. Exp. Med.* **213,** 329–339
22. Swamy, R. K., Manickam, J., Adhikari, J. S., and Dwarakanath, B. S. (2005) Glycolytic inhibitor, 2-deoxy-D-glucose, does not enhance radiation-induced apoptosis in mouse thymocytes and splenocytes *in vitro*. *Indian J. Exp. Biol.* **43,** 686–692
23. Miller, D. K. (1997) The role of the Caspase family of cysteine proteases in apoptosis. *Semin. Immunol.* **9,** 35–49
24. Budihardjo, I., Oliver, H., Lutter, M., Luo, X., and Wang, X. (1999) Biochemical pathways of caspase activation during apoptosis. *Annu. Rev. Cell Dev. Biol.* **15,** 269–290
25. Nakayama, M., Ishidoh, K., Kojima, Y., Harada, N., Kominami, E., Okumura, K., and Yagita, H. (2003) Fibroblast growth factor-inducible 14 mediates multiple pathways of TWEAK-induced cell death. *J. Immunol.* **170,** 341–348
26. Venugopal, B., and Evans, T. R. (2011) Developing histone deacetylase inhibitors as anti-cancer therapeutics. *Curr. Med. Chem.* **18,** 1658–1671
27. Marks, P. A., and Dokmanovic, M. (2005) Histone deacetylase inhibitors. Discovery and development as anticancer agents. *Expert Opin. Investig. Drugs* **14,** 1497–1511
28. Chuang, D. M., Leng, Y., Marinova, Z., Kim, H. J., and Chiu, C. T. (2009) Multiple roles of HDAC inhibition in neurodegenerative conditions. *Trends Neurosci.* **32,** 591–601
29. Monneret, C. (2007) Histone deacetylase inhibitors for epigenetic therapy of cancer. *Anticancer Drugs* **18,** 363–370
30. Marrack, P., and Kappler, J. (2004) Control of T cell viability. *Annu. Rev. Immunol.* **22,** 765–787
31. Veis, D. J., Sorenson, C. M., Shutter, J. R., and Korsmeyer, S. J. (1993) Bcl-2-deficient mice demonstrate fulminant lymphoid apoptosis, polycystic kidneys, and hypopigmented hair. *Cell* **75,** 229–240
32. Eischen, C. M., Woo, D., Roussel, M. F., and Cleveland, J. L. (2001) Apoptosis triggered by Myc-induced suppression of Bcl-X_L or Bcl-2 is bypassed during lymphomagenesis. *Mol. Cell. Biol.* **21,** 5063–5070
33. Hotchkiss, R. S., Swanson, P. E., Knudson, C. M., Chang, K. C., Cobb, J. P., Osborne, D. F., Zollner, K. M., Buchman, T. G., Korsmeyer, S. J., and Karl, I. E. (1999) Overexpression of Bcl-2 in transgenic mice decreases apoptosis and improves survival in sepsis. *J. Immunol.* **162,** 4148–4156
34. Marsden, V. S., and Strasser, A. (2003) Control of apoptosis in the immune system. Bcl-2, BH3-only proteins and more. *Annu. Rev. Immunol.* **21,** 71–105
35. Maksimow, M., Söderström, T. S., Jalkanen, S., Eriksson, J. E., and Hänninen, A. (2006) Fas costimulation of naive CD4 T cells is controlled by NF-κB signaling and caspase activity. *J. Leukocyte Biol.* **79,** 369–377
36. Takahashi, K., Miyatani, K., Yanai, H., Jeon, H. J., Fujiwara, K., Yoshino, T., Hayashi, K., Akagi, T., Tsutsui, K., and Mizobuchi, K. (1992) Induction of interdigitating reticulum cell-like differentiation in human monocytic leukemia cells by conditioned medium from IL-2-stimulated helper T-cells. *Virchows Arch. B. Cell Pathol. Incl. Mol. Pathol.* **62,** 105–113
37. Takahashi, I., Miyaji, H., Yoshida, T., Sato, S., and Mizukami, T. (1996) Selective inhibition of IL-2 gene expression by trichostatin A, a potent inhibitor of mammalian histone deacetylase. *J. Antibiot.* **49,** 453–457
38. Matsuoka, H., Fujimura, T., Mori, H., Aramori, I., and Mutoh, S. (2007) Mechanism of HDAC inhibitor FR235222-mediated IL-2 transcriptional repression in Jurkat cells. *Int. Immunopharmacol.* **7,** 1422–1432
39. Wang, Z., Leng, Y., Tsai, L. K., Leeds, P., and Chuang, D. M. (2011) Valproic acid attenuates blood-brain barrier disruption in a rat model of transient focal cerebral ischemia. The roles of HDAC and MMP-9 inhibition. *J. Cereb. Blood Flow Metab.* **31,** 52–57